

## BIOCHEMICAL CHARACTERIZATION OF XTHA AP-ENDONUCLEASE FROM *HELICOBACTER PYLORI*

Turgimbaeva A.M.<sup>1,2</sup>, Abeldenov S.K.<sup>1</sup>, Saparbayev M.K.<sup>3</sup>, Ramankulov Y.M.<sup>1</sup>,  
Khassenov B.B.<sup>1</sup>

<sup>1</sup>National Center for Biotechnology

13/5, Korgalzhyn road, Astana, 010000, Kazakhstan

<sup>2</sup>L.N. Gumilyov Eurasian National University

Satpayev Street, 2, Astana, 010000, Kazakhstan

<sup>3</sup>Institute of Gustav Roussy

CNRS UMR 8200, 114 Rue Edouard Vaillant, Villejuif, 94805, France

### ABSTRACT

About 50% of world population is infected by pathogenic bacterium *Helicobacter pylori*. During persistence in the human body, this microorganism encounters negative effects of reactive oxygen and nitrogen species (ROS, RNS) generated by neutrophils and macrophages, which damage bacterial DNA. Consequently, microorganism triggers a mechanism for eliminating DNA damages that is carried out by DNA repair enzymes. Base excision repair (BER) is one of the ways of DNA repair to eliminate oxidized, deaminated and alkylated nitrogenous bases. The key enzymes of BER are apurinic/apyrimidinic endonucleases (AP-endonucleases).

In this article research results of DNA repair activity of XthA AP-endonuclease from *H. pylori* (HpXthA) are presented. The optimal reaction conditions were determined for verifying the repair activity of HpXthA *in vitro*: low ionic strength, high concentration of Mg<sup>2+</sup>, pH 7-8 and 30°C incubation temperature. Kinetic parameters of AP-endonuclease, 3'-phosphodiesterase and 3'-phosphatase activity of HpXthA have been determined ( $k_{cat}/K_M = 1240, 44$  and  $5.4 \mu\text{M}^{-1} \cdot \text{min}^{-1}$ , respectively).

**Key words:** base excision repair, *Helicobacter pylori*, AP-endonuclease, AP-site, oxidative stress, oxidized DNA damage.

---

### INTRODUCTION

*Helicobacter pylori* is one of the most common pathogens, it inhabits in the gastric mucosa close to epithelial cells. *H. pylori* colonizes the human gastric mucosa about 50% of the world population. The presence of this microorganism in the stomach can cause gastritis, peptic ulcer and stomach cancer [1]. There are high rates of *H. pylori* infection of population in Kazakhstan. According to monitoring data for 2013, in Kazakhstan the prevalence of symptomatic and asymptomatic *H. pylori* infections was 76.5% [2, 3]. In 1994, the World Health Organization recognized *H. pylori* as a group I carcinogen [4].

During infection, all pathogens, including *H. pylori*, cause immune responses in the human body that lead to an "oxidative burst". It happens due to neutrophils and macrophages, that generate reactive oxygen and nitrogen species (ROS, RNS) in bulk [5,6]. Activated neutrophils and macrophages increase consumption of oxygen, which is reduced to the superoxide anion

(O<sub>2</sub><sup>•-</sup>) by NADPH-oxidase and moves to the phagosome. In the phagosome, superoxide anions are converted into other more destructive forms of oxygen, nitrogen and chlorine, causing DNA and protein damage of the pathogen [7,8]. In the case of the inability of phagocytes to destroy microorganisms, patients become susceptible to infections caused by certain bacteria and fungi [9]. The importance of this aspect is traced in people with chronic granulomatous disease. As a response, microorganisms trigger the mechanism eliminating DNA damage, carried out by DNA repair enzymes. One of the ways of DNA repair to correct oxidized, deaminated and alkylated bases is base excision repair (BER) pathway [10].

BER is initiated by DNA glycosylases that break the N-glycosidic bond between the damaged nitrogenous base and sugar to form an apurinic/aprimidinic site (AP site). AP sites can also occur due to spontaneous apurination of deoxyribonucleotides in the DNA [10, 11]. In turn, AP sites serve as substrates for AP endonucleases that hydrolyze the phosphodiester linkage directly at the 5'-phosphate group of the AP site and introduce a single-stranded DNA cleavage. Repair process is completed with the participation of AP-endonucleases, DNA polymerases and DNA ligases [11]. AP sites are cytotoxic, they block important physiological processes – replication and transcription; their timely elimination is necessary for the cell to survive [11, 12].

Elimination of AP sites is carried out by enzymes of BER pathway – AP-endonucleases of two families Nfo and XthA [11]. In comparison with *E. coli*, *M. tuberculosis* and *N. meningitidis*, *H. pylori* has only one AP-endonuclease – XthA [13], [14], which have not been studied yet.

The aim of this work is to determine the biochemical activity of XthA AP-endonuclease from *H. pylori* (HpXthA).

## **MATERIALS AND METHODS**

### **Strains, DNA, vectors and reagents**

Genomic DNA of *Helicobacter pylori* J99 was kindly provided by RSE "Republican collection of microorganisms" (Astana, Kazakhstan). Plasmid vectors pGEM-T (Promega) and pET28c (+) (Novagen) were used. Restriction endonucleases, T4 DNA ligase, Phusion High-fidelity DNA polymerase from Thermo Scientific were used for cloning and amplification of the target gene. Taq DNA polymerase of own preparation was used for PCR screening of transformed colonies [15]. *E. coli* strain DH5 $\alpha$  was used for cloning and plasmid preparation. *E. coli* strain Rosetta 2 (DE3) was used to express gene of HpXthA protein in heterologous conditions.

### **Media**

Low-salt Luria Bertani broth (1% tryptone, 0,5% yeast extract, 0,5% NaCl) was used for cultivation *E.coli* strains. SOC (2% tryptone, 0,5% yeast extract, 0,05% NaCl, 2,5 mM KCl, 20 mM MgSO<sub>4</sub>, 20 mM glucose, pH 7.5) medium was used for incubation of the transformed cells. In the media the concentration of kanamycin and ampicillin was 50  $\mu$ g/ml and 150  $\mu$ g/ml, respectively. The preparation of media was carried out in accordance with standard protocol [16].

### **Oligonucleotides**

Oligonucleotides listed in table 1 were used for cloning and sequencing of *xthA* gene from *H. pylori*.

**Table 1.** Oligonucleotides for cloning

Oligonucleotide	Sequence
5NdeI-HpXthA	5'-GGGAATTCCATATGAAACTGATTTTCATGGAATGTGAAC-3'
3BamHI-HpXthA	5'-CGCGGATCCGTTAAACTAATTCCAACCTACCGG-3'
5HpXthA_D144N	5'-GTCATTGTGTGTGGGA <u>AACTT</u> GAAATGTGGCCC-3'
3HpXthA_D144N	5'-GGGCCACATTCAAG <u>TTCCC</u> CACACACAATGAC-3'
T7fw	5'-TAATACGACTCACTATAGGG-3'
T7rv	5'-GCTAGTTATTGCTCAGCGG-3'
M13fw	5'-GTAAAACGACGGCCAG-3'
M13rv	5'-CAGGAAACAGCTATGAC-3'

Note – in the sequence of 5HpXthA\_D144N primer asparagine codon is highlighted, which replaces codon of aspartic acid; in 3HpXthA\_D144N primer – complementary triplet of asparagine codon.

### Amplification and cloning of *xthA* gene from *H. pylori* into expression vectors

PCR conditions for amplification of target gene from *H. pylori* genomic DNA: 100 ng *H. pylori* genomic DNA, 0.2  $\mu$ M of each primer (5NdeI-HpXthA and 3BamHI-HpXthA), 0.2  $\mu$ M dNTP mix (2.5 mM of each), 1x HF buffer (containing 1.5 mM MgCl<sub>2</sub>), 1.5 mM MgCl<sub>2</sub>, 3% DMSO, Phusion High-fidelity DNA polymerase (2 units). PCR cycling regime: +98°C – 1 min; 35 cycles: +98°C – 15 seconds, +55°C – 30 seconds, +72°C – 40 seconds; +72°C – 5 min. The amplified *xthA* gene from *H. pylori* was purified by phenol-chloroform extraction and cloned into the pGEM-T vector, according to manufacturer's protocol. Plasmid DNA was isolated using the MiniPrep kit (Thermo Scientific).

For cloning into pET28c (+) expression vector, *xthA* gene from *H. pylori* was amplified from pGEM-T/HpXthA plasmid: 135 ng pGEM-T/HpXthA, 0.8 mM dNTP mix, 0.2  $\mu$ M of each primer (5NdeI- HpXthA and 3BamHI-HpXthA), 1x HF buffer (containing 1.5 mM MgCl<sub>2</sub>), Phusion High-fidelity DNA polymerase (1 unit). PCR cycling regime is similar to above mentioned, except for cycle number - 30 cycles. Amplified *xthA* gene from *H. pylori* was purified by phenol-chloroform extraction, after which obtained gene and expression vector were digested by *NdeI* and *BamH I* restriction enzymes in 2X Tango buffer. Ligation was performed by T4 ligase in T4 ligase buffer for 16 hours at +4°C.

Competent DH5 $\alpha$  cells were transformed with the resulting ligase mixture by temperature shock method. Selection of transformed colonies was carried out on 1.5% LB agar with kanamycin, followed by PCR screening in T7 region. Positive colonies were inoculated into LB broth with kanamycin for further isolation of plasmid. The integrated insert was sequenced by Sanger method using T7 primers and compared with reference sequence from GenBank database: CP011330.1 (range: 1144587-1145339).

### Site-directed mutagenesis

Site-directed mutagenesis was performed in pET28c(+)/HpXthA expression vector to obtain mutant protein with amino acid substitution D144N. Site-directed mutagenesis was performed using QuickChange site-directed mutagenesis kit (Stratagene) and 5HpXthA\_D144N and 3HpXthA\_D144N primers. As a result, pET28c(+)/HpXthA D144N expression vector was obtained.

## Immobilized metal ion affinity chromatography of HpXthA recombinant protein

Competent cells of *E. coli* Rosetta 2 (DE3) strain were transformed by obtained pET28c(+)/HpXthA and pET28c(+)/HpXthA D144N vectors. A single transformed colony was inoculated into LB broth with kanamycin. In the middle of the logarithmic growth phase of bacterial culture ( $OD_{600}=0.6$ ), isopropyl- $\beta$ -D-1-thiogalactopyranoside (IPTG) was added at a final concentration of 0.5 mM. The culture was incubated at room temperature and 100 rpm shaking for 16 hours. The night culture was harvested at + 4°C, 6000×g for 7 minutes. The pellet was resuspended in 20 mM NaCl, 20 mM Tris-HCl pH 8.0 buffer with a protease inhibitors cocktail (Roche Diagnostics). The cells were lysed by a French Press (Thermo) at 124 MPa pressure, then it was sonicated at 10 kHz frequency. Cell lysate was centrifuged at + 4°C, 40000×g for 60 minutes. NaCl concentration was adjusted to 500 mM in the clarified lysate. The clarified lysate was loaded onto a HiTrap Chelating HP (GE Healthcare) column pre-activated by Ni<sup>2+</sup> ions. Recombinant protein was fractionated in a linear gradient of imidazole concentrations from 20 mM to 500 mM using a FPLC AKTA Purifier 10 (GE Healthcare) chromatograph. Obtained fractions with target protein were combined and loaded into a HiTrap Heparin HP (GE Healthcare) column. The fractions were eluted in a linear NaCl gradient from 50 mM to 1M. The homogeneity of the obtained fractions was checked by separation in 12% of SDS-PAGE. Samples were stored at -20°C in 50% glycerol.

## Oligonucleotides of DNA duplexes

All used oligodeoxyribonucleotides containing modified residues and their complementary oligonucleotides were produced by Eurogentec.

The following oligonucleotides were used to determine the substrate-specificity of the enzyme: 30mer X-RT d(TGACTGCATAXGCATGTAGACGATGTGCAT), where X – tetrahydrofuran (THF, synthetic analogue of AP site),  $\alpha$ -2'-deoxyadenosine ( $\alpha$ dA), 5-hydroxycytosine (5ohC) or 5,6-dihydrouracil (DHU), and a complementary 30-mer oligonucleotide containing dA, dG, dC and dT opposite the lesion. The context DNA sequence was previously used for DNA substrate characteristics of *Escherichia coli*, *Saccharomyces cerevisiae*, *Mycobacterium tuberculosis* and *Triticum aestivum* [17, 18, 19].

Oligonucleotides were labeled with a radioactive label either from the 5'-end with the T4 polynucleotide kinase (New England Biolabs) in the presence of [ $\gamma$ -<sup>32</sup>P]ATP (3000 Ci • mmol<sup>-1</sup>) (PerkinElmer SAS), or at the 3'-end with terminal transferase (New England Biolabs) in the presence of [ $\alpha$ -<sup>32</sup>P]3'dATP (cordycepin 5'-triphosphate, 5000 Ci • mmol<sup>-1</sup>) (PerkinElmer), according to manufacturers' recommendations. Annealing of labeled oligonucleotides with relevant complementary oligonucleotides is carried out in a buffer containing 50 mM KCl and 20 mM HEPES-KOH (pH 7.5), at 65°C for 3 minutes. Annealing was followed by cooling for 2 hours till room temperature. The resulting DNA substrates were called X•C (G, A, T), respectively, where X is the modified residue.

The following nucleotides were used to measure 3'→5' exonuclease, 3'-phosphodiesterase and 3'-phosphatase activities: Exo20 d(GTGGCGCGGAGACTTAGAGA); Exo20<sup>THF</sup> d(GTGGCGCGGAGACTTAGAGAX), where X – 3'-terminal THF; Exo20p d(GTGGCGCGGAGACTTAGAGAp), where p – 3'-terminal phosphate group; 5P-Exo19 d(pATTTGGCGCGGGGAATTCC), where p – 5'-terminal phosphate group; and complementary oligonucleotide Rex-T d(GGAATCCCCGCGCCAAATTTCTCTAAGTCTCCGCGCCAC), containing T opposite the THF. To determine the 3'-phosphatase activity, Exo20 oligonucleotide was labeled at the 3'-end with [ $\alpha$ -<sup>32</sup>P]3'dATP by cordycepin to create a Exo20-3'-dAM<sup>32</sup>p 21mer, which was then treated with recombinant Tdp1 (courtesy of professor Olga Lavrik, Novosibirsk, Russia). Obtained Exo20-3'-<sup>32</sup>P 20mer was annealed with complementary Rex-T oligonucleotide and was used together with unlabeled Exo20p • RexT duplex.

## Determination of AP endonuclease activity using synthetic DNA duplexes

To determine AP-endonuclease activity of HpXthA 20  $\mu$ l reaction mixture was used. It contained 10 nM [ $^{32}$ P]-labelled DNA duplex, 50 mM Tris-HCl (pH 8.0), 25 mM KCl, 5 mM MgCl<sub>2</sub>, 0.05 mM DTT, 100  $\mu$ g/ml BSA, 0.01% of Nonidet P-40 and 0.2 nM enzyme. The reaction mixture was incubated at +30°C for 5 minutes. To measure the kinetic parameters of 3'→5' exonuclease activity 10-6000 nM DNA duplex was incubated in the previously described reaction conditions. Kinetic constants and  $K_M$  and  $k_{cat}$  values were calculated using Prism4 software (GraphPad Software). The kinetic parameters of 3'→5' exonuclease were computed by measuring the reaction products signified as a percentage of the total substrate. If multiple DNA products were formed, the values of each degradation product were multiplied by the number of catalytic decompositions necessary for its formation. Then the total exonuclease activity was calculated by summing all products.

The reaction was stopped by 10  $\mu$ l stop buffer (0.5% SDS, 20 mM EDTA), the reaction products were desalted on Sephadex G25 column (Amersham Biosciences), equilibrated with 7.5 M urea and 0.05% bromophenol blue. Desalted reaction products were separated in a 20% denaturing polyacrylamide gel with 7.5 M urea. After electrophoresis gel was scanned by Fuji FLA 9500 Phosphor Imager (GE Healthcare life sciences), the results were analyzed by Image Gauge V4.0 program. At least 3 independent experiments were hold for all kinetic measurements.

## RESULTS AND DISCUSSION

### Gene amplification and cloning into expression vectors

Reference sequence CP011330.1 of *H. pylori xthA* gene from GenBank database was used for design of gene-specific primers, gene length is 750 bp. The amplified PCR product from genomic DNA of *H. pylori* is shown in figure 1.

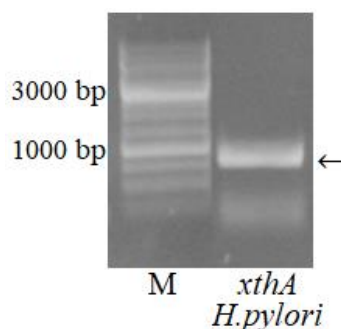


**Fig. 1.** Amplified *xthA* gene from genomic DNA of *H. pylori*

After transformation of *E. coli* DH5 $\alpha$  strain cells with obtained pGEM-T/HpXthA plasmid, positive clones were selected by blue-white screening, the insert was sequenced by M13 primers. Sequencing of positive clones by Sanger method and comparison with the reference sequence showed that identity of nucleotide and amino acid sequences for *xthA* gene from *H. pylori* is 99%. A polymorphism in the form of one amino acid substitution G181 → D181 was established in comparison with the reference sequence from Genbank.

The received gene was cloned from pGEM-T/HpXthA plasmid into pET28c(+) expression vector at *Nde*I and *Bam*HI restriction sites, it was inserted under the control of T7 promoter. The sequencing confirmed absence of mutations in the open reading frame of pET28c/HpXthA expression vector. The resulting protein contained an additional 20 amino acid domain at the N-

terminus containing a six-histidine tag and a thrombin cleavage site. Thus, recombinant HpXthA protein consisted of 270 amino acid residues, with a total molecular weight of 30.2 kDa

### Immobilized metal ion affinity chromatography of HpXthA recombinant protein

During purification by immobilized metal ion affinity chromatography (IMAC) HpXthA protein eluted at 220 mM imidazole, during purification on heparin column HpXthA eluted at 345 mM NaCl (Figure 2). The final yield of the purified protein was 1 mg from a 200 ml culture.

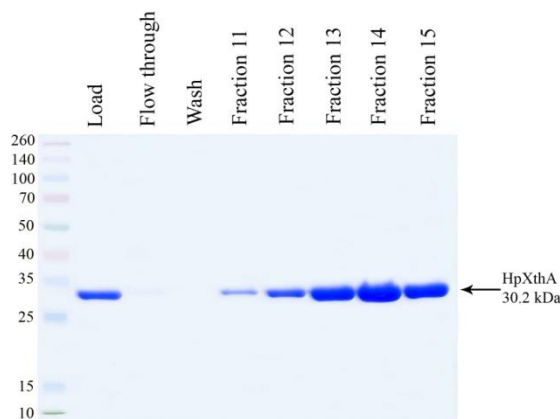


**Fig. 2.** Electrophoregram of purification of recombinant HpXthAAP-endonuclease on heparin

pET28c/HpXthA D144N genetic construct was obtained by site-directed mutagenesis. There is *xthA* gene from *H. pylori* with a point mutation leading to the replacement of aspartic acid by asparagine in the 144<sup>th</sup> position (D144N) in pET28c/HpXthA D144N. Purification of mutant HpXthA D144N protein was carried out by metal-affinity chromatography on a HiTrap Chelating HP column activated by Ni<sup>2+</sup> ions (figure 3).

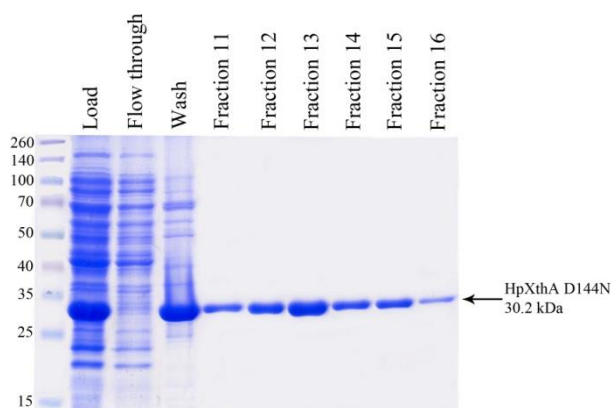


**Fig. 3.** Electrophoregram of purification of recombinant HpXthA D144N AP-endonuclease by IMAC

The resulting recombinant proteins have a high electrophoretic purity, which is sufficient for use in experiments for determination their DNA repair activity. Tetrahydrofuran (THF), acting as a synthetic analogue of AP site, was used to determine AP-endonuclease activity of enzyme [20].

### Biochemical characteristic of the enzyme

It is known that ExoIII family AP endonucleases of *E. coli* (XthA) and human (APE1) require presence of divalent cations of Mg<sup>2+</sup> for their catalytic activity [21,22]. There was detected Mg<sup>2+</sup>-dependent AP-endonuclease activity in the cell-free extract of *H. pylori*, that was

caused by homologue of *E. coli* XthA [23]. Therefore, in order to optimize the reaction conditions, AP-endonuclease activity of purified recombinant HpXthA was studied in the presence of different divalent cations ( $\text{MgCl}_2$ ,  $\text{MnCl}_2$ ,  $\text{CaCl}_2$ ,  $\text{CoCl}_2$ ,  $\text{ZnCl}_2$ ,  $\text{NiCl}_2$  и  $\text{FeCl}_2$ ,  $\text{CuSO}_4$ ). 5'- $^{32}\text{P}$ -labeled THF•T duplex, containing tetrahydrofuran (THF) at the 11<sup>th</sup> position, was used as substrate for HpXthA (figure 4).

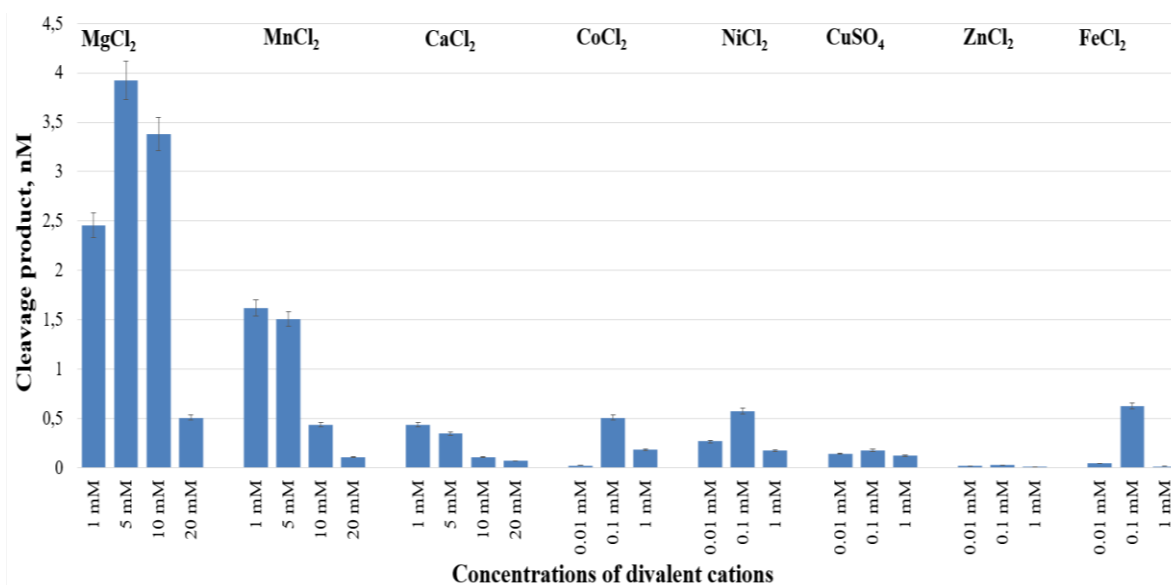


**Fig. 4.** Dependence of AP-endonuclease activity of HpXthA on the concentrations of divalent metal cations

As shown in Figure 4, AP-endonuclease activity of HpXthA is the most effective at 5 mM  $\text{MgCl}_2$ . However, as the concentration of  $\text{Mg}^{2+}$  cations (10-20 mM) increases, the activity of the enzyme decreases. At 1-5 mM  $\text{MnCl}_2$  the enzyme is active, but lower in comparison with activity at the same molar concentration of  $\text{MgCl}_2$ . HpXthA loses AP-endonuclease activity at increasing concentrations of  $\text{MnCl}_2$  (10-20 mM). An extremely low activity of the enzyme is observed with increasing concentrations of  $\text{MnCl}_2$  (10-20 mM), HpXthA loses AP-endonuclease activity. An extremely low activity of the enzyme is observed at 1-20 mM  $\text{CaCl}_2$ . Low AP-endonuclease activity of HpXthA is detected in the presence of  $\text{CoCl}_2$ ,  $\text{ZnCl}_2$ ,  $\text{NiCl}_2$  and  $\text{FeCl}_2$ ,  $\text{CuSO}_4$ . The graph of activity dependence on concentrations of divalent cations  $\text{Co}^{2+}$ ,  $\text{Ni}^{2+}$ ,  $\text{Fe}^{2+}$  has a bell-shaped appearance. Concentration increase of  $\text{CuSO}_4$  and  $\text{ZnCl}_2$  leads to activity inhibition of HpXthA. Thus, HpXthA is a metal-specific protein with maximum activity at 5 mM  $\text{MgCl}_2$ .

Parameters of buffer solution (concentration of  $\text{MgCl}_2$  and  $\text{KCl}$ , pH) and the incubation temperature were optimized for further experiments (figure 5). THF•T duplex was used as a substrate.

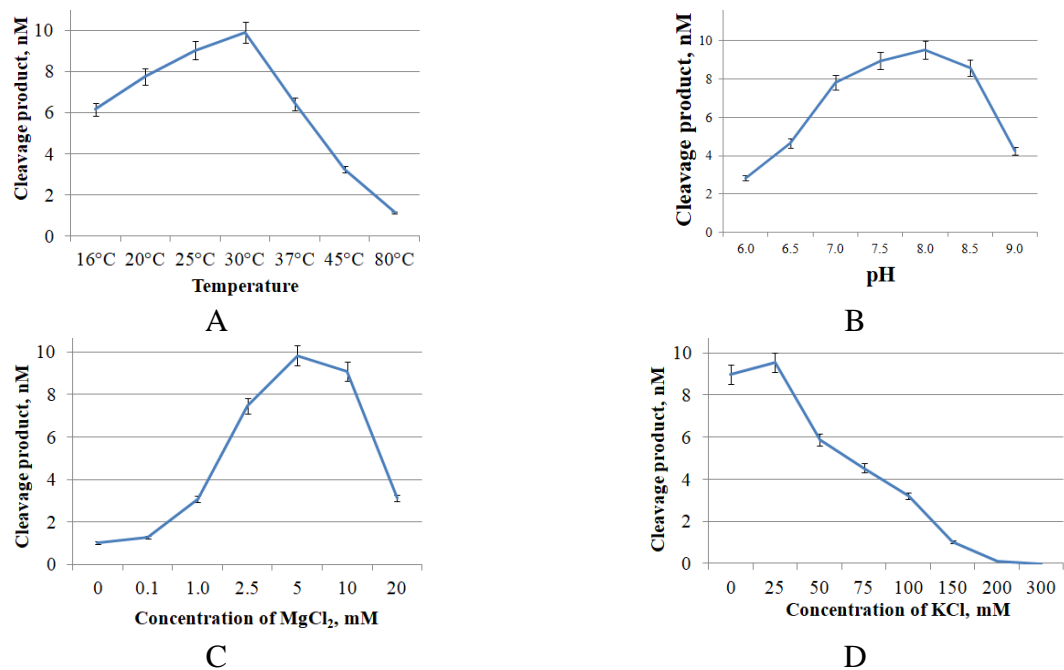


**Fig. 5.** Graphs of dependence of HpXthA's AP-endonuclease activity on temperature (A), pH (B), concentration of Mg<sup>2+</sup> ions (C) and KCl (D)

According to figure 5, graphs of dependence of HpXthA's AP-endonuclease activity on temperature, pH, concentration of MgCl<sub>2</sub> and KCl are bell-shaped. The highest level of activity of HpXthA AP-endonuclease was observed in the following conditions: 25 mM KCl, 50 mM Tris-HCl pH 8.0, 5 mM MgCl<sub>2</sub>, incubation temperature +30°C. These reaction conditions with a low concentration of KCl and a relatively high concentration of Mg<sup>2+</sup> are more similar to those of *E. coli* XthA [22] than human APE1 [24].

Mutant HpXthA D144N protein was obtained by site-directed mutagenesis to confirm DNA repair activity of obtained recombinant HpXthA protein and to exclude DNA repair activity of *E. coli* XthA and Nfo enzymes. Aspartic acid (D) was replaced by asparagine (N) in the 144<sup>th</sup> position of amino acid sequence of explored enzyme. Choice of this amino acid substitution is based on fact that D210N replacement in homologous human APE1 AP-endonuclease lead to 10,000-fold decrease in activity [25]. It is known that Asp210 coordinates the metal-binding site of the enzyme [26], which is important for implementation of AP-endonuclease activity. Purified recombinant wild-type (WT) HpXthA and HpXthA D144N proteins were incubated with 5'-[<sup>32</sup>P]-labelled THF•T and Exo20•RexT<sup>Rec</sup> duplexes to measure AP-endonuclease and 3'→5' exonuclease activities. The reaction was carried out in an optimized buffer at 30°C for 5 minutes (figure 6).

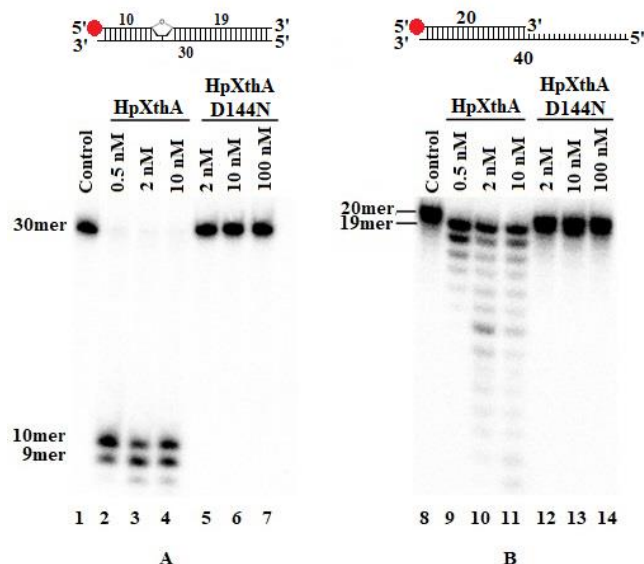
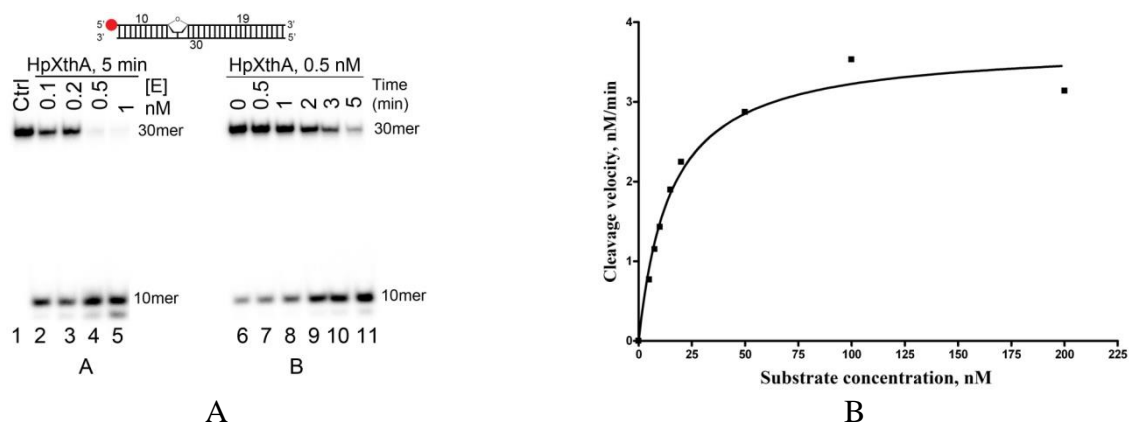


**Fig. 6.** Comparative analysis of AP-endonuclease (A) and 3'→5' exonuclease (B) activities of HpXthA WT and HpXthA D144N

As seen in Figure 6, AP-endonuclease (lanes 2-4) and 3'→5' exonuclease (tracks 8-11) activities are observed at 0.5 nM, 2 nM, and 10 nM HpXthA. In the case of AP endonuclease activity, THF in the 11<sup>th</sup> position is cleaved by enzyme. As a result, there is migration of radio-labeled 10-mer product, which is disintegrated to 9- and 8-mers. In the case of 3'→5' exonuclease activity, the substrate degradation products of HpXthA WT are seen as a ladder. Despite the large concentrations of HpXthA D144N (2 nM, 10 nM, 100 nM), cleavage of the initial duplexes does not occur (lanes 5-7, 12-14) in comparison with HpXthA WT. This confirms the absence of contamination by native *E. coli* AP endonucleases in tested recombinant HpXthA protein.

To determine the kinetic parameters of AP-endonuclease activity, 10 nM 5'-[<sup>32</sup>P]-labeled THF•T duplex was incubated at 30°C with different concentrations of HpXthA (lanes 2-5) for 5 minutes and with the optimal concentration of HpXthA (0.5 nM) for 0.5, 1, 2, 3 and 5 minutes (lanes 6-10). 10 nM 5'-[<sup>32</sup>P]-labeled THF•T duplex in reaction mixture was used as a negative control (figure 7).



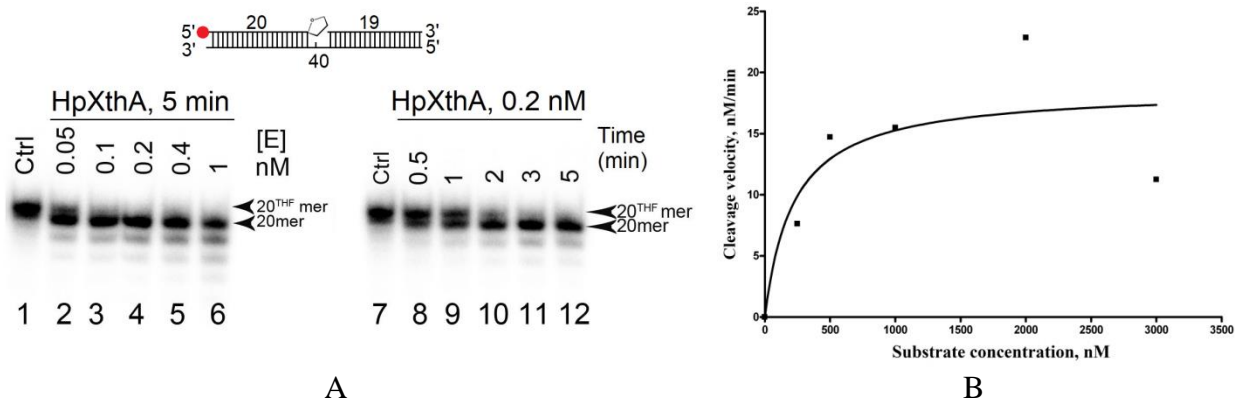
A – analysis of reaction products in a denaturing polyacrylamide gel; B – graphical representation of kinetics

**Fig. 7.** Kinetics of THF•T cleavage by HpXthA

According to Figure 7, 10-mer products of the initial substrate (lanes 2-10) are generated during incubation of THF•T with HpXthA, indicating the presence of AP endonuclease activity.

HpXthA demonstrates effective cleavage activity of AP-site: 0.5 nM HpXthA can cleave >95% 10 nM oligonucleotide substrate for 5 minutes in selected experimental conditions (lanes 4 and 10). After incubation THF•T with 1 nM HpXthA, 9-mers are generated (lane 5). 9-mers are products of 10-mer cleavage caused by 3' → 5' exonuclease activity of enzyme.

To determine the kinetic parameters of 3'-phosphodiesterase activity, 10 nM 5'-[<sup>32</sup>P]-labeled Exo20<sup>THF</sup>•RexT<sup>Nick</sup> duplex was incubated with different concentrations of HpXthA (lanes 2-6) for 5 minutes at 30°C and with the optimal concentration of HpXthA (0.2 nM) for 0.5, 1, 2, 3 and 5 minutes (lanes 8-12). 10 nM 5'-[<sup>32</sup>P]-labeled Exo20<sup>THF</sup>•RexT<sup>Nick</sup> duplex in reaction mixture was used as a negative control (figure 8).

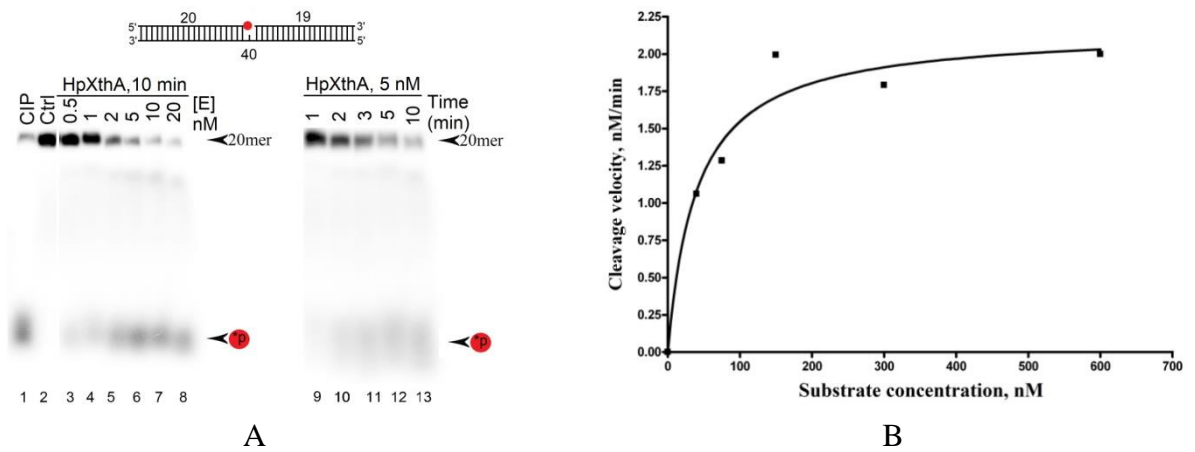


A – analysis of reaction products in a denaturing polyacrylamide gel; B – graphical representation of kinetics

**Fig. 8.** Kinetics Exo20<sup>THF</sup>•RexT<sup>Nick</sup> cleavage by HpXthA

As shown in Figure 8, HpXthA cleaves 5'-[<sup>32</sup>P]-labeled Exo20<sup>THF</sup>•RexT<sup>Nick</sup> duplex: 20-mer DNA fragment is formed that migrates faster than the 20-mer Exo20<sup>THF</sup> substrate. Enzyme removes the 3-terminal THF-residue to form Exo20 fragment with the 3'-OH end (lanes 2-6 and 9-12). HpXthA removes the 3'-THF residue in >90% duplex molecules of Exo20<sup>THF</sup>•RexT<sup>Nick</sup> in 5 minutes (lane 2) even at low concentrations (0.05 nM), while 0.2 nM HpXthA cleaves the greatest part of DNA substrate after 2 minutes of incubation (lane 10). This suggests that XthA of *H.pylori* has a highly effective 3'-phosphodiesterase activity along with AP-endonuclease activity.

To determine the kinetic parameters of 3'-phosphatase activity, 10 nM 5'-[<sup>32</sup>P]-labeled Exo20<sup>P</sup>•RexT<sup>Nick</sup> duplex was incubated with different concentrations of HpXthA (lanes 3-8, figure 9) for 10 minutes at 30°C and with the optimal concentration HpXthA for 1, 2, 3, 5 and 10 minutes (lanes 9-13, figure 9). 10 nM 5'-[<sup>32</sup>P]-labeled Exo20<sup>P</sup>•RexT<sup>Nick</sup> duplex in reaction buffer was used as a negative control (lane 2). For comparison with a positive control, 10 nM 5'-[<sup>32</sup>P]-labeled Exo20<sup>P</sup>•RexT<sup>Nick</sup> duplex was treated with calf intestinal alkaline phosphatase (CIP, lane 1).

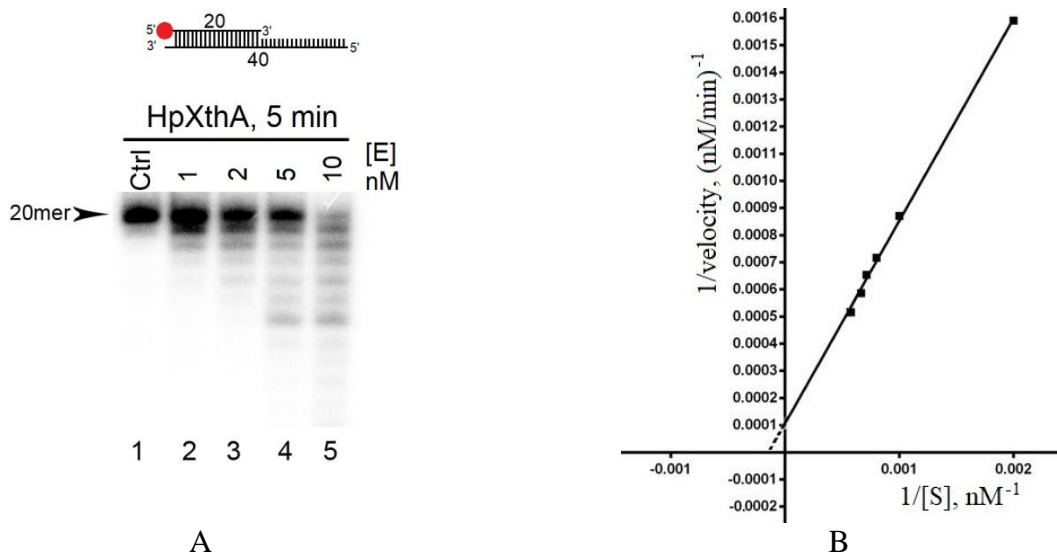


A – analysis of reaction products in a denaturing polyacrylamide gel; B – graphical representation of kinetics

**Fig. 9.** Kinetics Exo20<sup>P</sup>•RexT<sup>Nick</sup> cleavage by HpXthA

After cleavage of 3'-[<sup>32</sup>P]-labeled Exo20<sup>P</sup>•RexT<sup>Nick</sup> duplex by HpXthA enzyme, free radioactive phosphate residues [<sup>32</sup>P] are formed (lanes 3-8). As a result of substrate cleavage, the 3'-terminal [<sup>32</sup>P] residues and Exo20 fragments migrate in the gel. It was found that higher concentration of HpXthA (5 nM) and longer incubation time (10 min) are required for removing >50% phosphate residues from Exo20<sup>P</sup>•RexT<sup>Nick</sup> duplex (lanes 6 and 12) in comparison to the Exo20<sup>THF</sup> substrate.

In addition to above mentioned activities, AP-endonucleases of XthA family have 3'-5' exonuclease activity, biological role of which remains unclear [27]. For determination of the kinetic parameters of 3'-5'-exonuclease activity, duplex mixtures (10 nM 5'-[<sup>32</sup>P]-labeled Exo20•RexT and 10 nM Exo20•RexT) was incubated with 1, 2, 5 and 10 nM HpXthA (lanes 2-5, figure 10) for 5 minutes at 30°C. 10 nM 5'-[<sup>32</sup>P]-labeled Exo20•RexT duplex in reaction mixture was used as a negative control (lane 1).



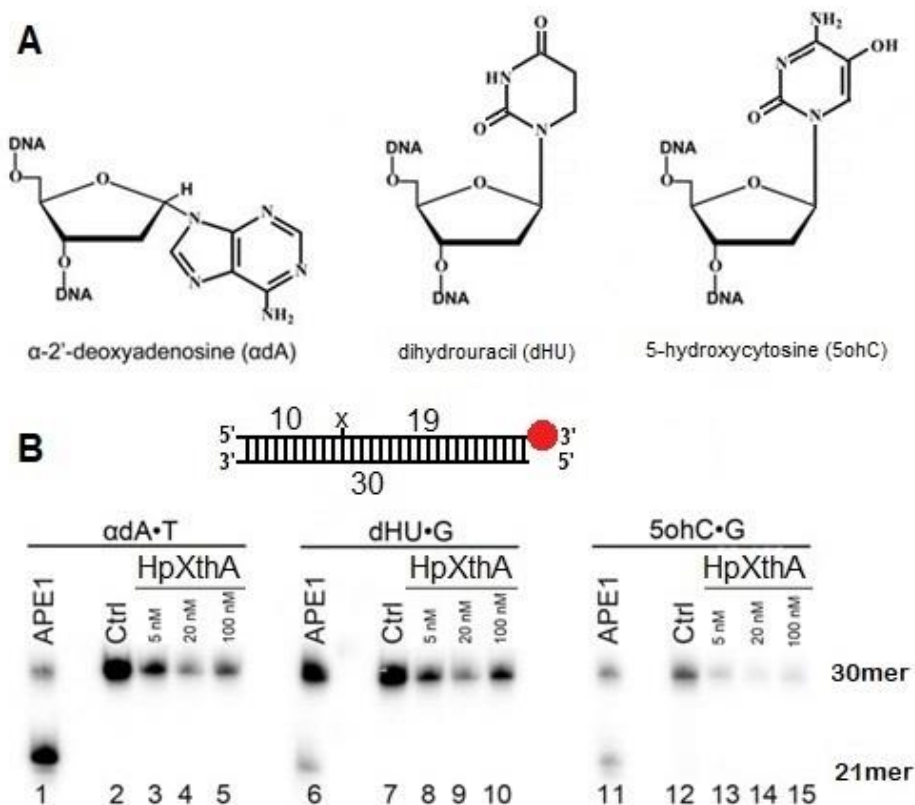
A – analysis of reaction products in a denaturing polyacrylamide gel; B – graphical representation of kinetics

**Fig. 10.** Kinetics Exo20•RexT cleavage by HpXthA

As seen in Figure 10, ladder of reaction products (lanes 2-5) is formed after cleavage of 5'-[<sup>32</sup>P]-labeled Exo20•RexT by HpXthA. For further analysis Lineweaver–Burk plot was built for 3'-5' exonuclease activity of HpXthA AP-endonuclease (figure 10B).

There are published data on mice insensitivity to oxidative agents with knocked-out DNA glycosylases, eliminating oxidized DNA damage in literary source [27]. Mutant strains of *Escherichia coli* and *Saccharomyces cerevisiae* without specific for oxidized DNA bases DNA glycosylase/AP-lyases are not sensitive to oxidizing agents and ionizing radiation [28, 29, 30, 31]. These results contradict the classical understanding of molecular mechanisms of BER pathway and suggest the existence of alternative pathways, one of which is nucleotide incision repair (NIR) [32]. This pathway implies DNA glycosylase-independent incision of oxidized DNA bases by AP-endonucleases. According to this mechanism, regardless of DNA glycosylase, AP endonuclease forms a single-stranded DNA break alongside the oxidized damage. As a result, correct ends are generated at 5'-end from modified nucleotide for the following DNA synthesis. It has been observed that certain types of DNA damage (UV-induced DNA photoadducts, alpha-anomeric nucleotides and oxidized bases) can be repaired by AP endonucleases without DNA glycosylases [32].

The specificity of HpXthA AP-endonuclease to the damaged nucleotides ( $\alpha$ -anomer of 2'-deoxyadenosine ( $\alpha$ dA), 5,6-dihydrouracil (DHU) and 5-hydroxycytosine (5ohC), included in 3'-[<sup>32</sup>P]-labeled 30-mer duplexes) was tested (figure 11). Cordycepin (3'-deoxyadenosine 5'-triphosphate, 3'-dATP) with [ $\alpha$ -<sup>32</sup>P]-label was attached by terminal transferase TdT to 30-mer substrate. If enzyme successfully cleaves DNA damage, 21-mer product is observed.



A – chemical structure of DNA damage, B – cleavage of DNA damage by HpXthA in denaturing polyacrylamide gel

**Fig. 11.** Detection of NIR activity of HpXthA AP endonuclease

According to figure 11, control enzyme APE1, for which the NIR activity was detected [32], cleaved duplexes with the following formation of 21-mer product containing  $\alpha$ dA•T, DHU•G

and 5ohC•G (lanes 1,6 and 11). At the same time, HpXthA did not cleave the initial substrates (lanes 3-5, 8-10, and 13-15), indicating the absence of NIR activity of HpXthA AP-endonuclease in these experimental conditions.

Based on obtained data, the kinetic parameters ( $K_M$ ,  $k_{cat}$ ,  $k_{cat}/K_M$ ) of DNA repair activities of HpXthA were calculated. Comparative analysis with already known data for AP-endonuclease of *E. coli* [19, 33], *H. sapiens* [21] and *M. tuberculosis* [19] allowed us to establish ratios of  $k_{cat}/K_M$ . HpXthA has equal AP-endonuclease activity as *E. coli* XthA and 10 times less effective than human APE1. In addition, HpXthA significantly exceeds AP-endonuclease activity of *M. tuberculosis* XthA (MtbXthA) (table 2).

**Table 2.** Comparison of the kinetic parameters of *E. coli*, *H. pylori*, *M. tuberculosis* and *H. sapiens* AP-endonucleases

DNA substrate	Enzyme						
	<i>H. pylori</i> XthA			<i>E. coli</i> XthA			
	$K_M$ , nM	$k_{cat}$ , min <sup>-1</sup>	$k_{cat}/K_M$ , μM <sup>-1</sup> ·min <sup>-1</sup>	$K_M$ , nM	$k_{cat}$ , min <sup>-1</sup>	$k_{cat}/K_M$ , μM <sup>-1</sup> ·min <sup>-1</sup>	$k_{cat}/K_M$ ratio, EcXthA/ HpXthA
THF•T	15.0 ± 2.2	18.5	1236	31	40	1300	1
Exo20 <sup>THF</sup> •RexT <sup>Nick</sup>	202± 100	8.8	43.6	731	32.2	44	1
Exo20 <sup>P</sup> •RexT <sup>Nick</sup>	40 ±14	0.22	5.4	-	-	-	-
Exo20•RexT <sup>Rec</sup>	6800 ± 1000	920 ± 140	135	-	-	-	-
DNA substrate	<i>H. pylori</i> XthA			Human APE1			
	$K_M$ , nM	$k_{cat}$ , min <sup>-1</sup>	$k_{cat}/K_M$ , μM <sup>-1</sup> ·min <sup>-1</sup>	$K_M$ , nM	$k_{cat}$ , min <sup>-1</sup>	$k_{cat}/K_M$ , μM <sup>-1</sup> ·min <sup>-1</sup>	$k_{cat}/K_M$ ratio, APE1/HpXthA
THF•T	15.0± 2.2	18.5	1236	7.7	97	12,700	10.3
Exo20 <sup>THF</sup> •RexT <sup>Nick</sup>	202± 100	8.8	43.6	6.0	20	3300	75.7
Exo20 <sup>P</sup> •RexT <sup>Nick</sup>	40±14	0.22	5.4	20	3.6	180	33.3
Exo20•RexT <sup>Rec</sup>	6800± 1000	920± 140	135	2.4	0.86	360	2.7
DNA substrate	<i>H. pylori</i> XthA			<i>M. tuberculosis</i> XthA			
	$K_M$ , nM	$k_{cat}$ , min <sup>-1</sup>	$k_{cat}/K_M$ , μM <sup>-1</sup> ·min <sup>-1</sup>	$K_M$ , nM	$k_{cat}$ , min <sup>-1</sup>	$k_{cat}/K_M$ , μM <sup>-1</sup> ·min <sup>-1</sup>	$k_{cat}/K_M$ ratio, MtbXthA/ HpXthA
THF•T	15.0± 2.2	18.5	1236	55.6± 19.2	0.025	0.45	0.0004
Exo20 <sup>THF</sup> •RexT <sup>Nick</sup>	202± 100	8.8	43.6	817± 226	362	443	10.2
Exo20 <sup>P</sup> •RexT <sup>Nick</sup>	40±14	0.22	5.4	571± 96	728	1275	236.1
Exo20•RexT <sup>Rec</sup>	6800± 1000	920± 140	135	1268± 362	6.4	5	0.04

Phosphodiesterase activity of HpXthA is equivalent to the activity of *E. coli* XthA and 76 and 10 times lower than the activity of homologues of human APE1 and MtbXthA, respectively. Phosphatase activity of HpXthA is 33 and 236 times inferior to APE1 and MtbXthA enzymes, respectively. Exonuclease activity of HpXthA is 2.7 times lower than that of human APE1, but it is 27 times higher than that of MtbXthA. Therefore, BER is a highly conserved physiological process found in both prokaryotes and eukaryotes, but AP endonucleases have a certain specificity in each organism. In particular, individual pathogenesis mechanism and the habitat of pathogen influence on enzyme specificity.

## CONCLUSION

In this study *xthA* gene was amplified from *H. pylori* genomic DNA in pET28c(+) expression vector to obtain pET28c (+)/HpXthA genetic construct. Recombinant HpXthA enzyme was obtained by metal-affinity chromatography. The absence of intrinsic AP-endonucleases of *E. coli* in studied enzyme was confirmed by experiments with mutant HpXthA D144N AP endonuclease. The kinetic parameters of AP-endonuclease, 3'-phosphodiesterase and 3'-phosphatase activities of HpXthA were determinate in selected optimal conditions (25 mM KCl, 50 mM Tris-HCl pH 8.0, 5 mM MgCl<sub>2</sub>, incubation temperature +30°C):  $k_{cat}/K_M = 1240$ , 44 and  $5.4 \mu\text{M}^{-1} \cdot \text{min}^{-1}$ , respectively. It was found that unlike *E. coli*, XthA from *H. pylori* does not have NIR activity.

It was established that XthA AP-endonuclease from *H. pylori* is a substrate-specific enzyme and plays a key role in elimination of damaged nitrogenous DNA bases.

## Acknowledgements

This work was supported by the Ministry of Education and Science of the Republic of Kazakhstan (grant №AP05130820 for 2018-2020 years).

## REFERENCES

1. Bauer B., Meyer T.F., Bauer B., Meyer T.F. The human gastric pathogen *Helicobacter pylori* and its association with gastric cancer and ulcer disease. *Ulcers*, 2011, vol. 2011, pp. 1-23.
2. Benberin V., Bektayeva R., Karabayeva R., Lebedev A., Akemeyeva K., Paloheimo L., Syrjänen K. Prevalence of *H. pylori* infection and atrophic gastritis among symptomatic and dyspeptic adults in Kazakhstan. A hospital-based screening study using a panel of serum biomarkers. *Anticancer Res.*, 2013, vol. 33, no. 10, pp. 4595-4602.
3. Eusebi L.H., Zagari R.M., Bazzoli F. Epidemiology of *Helicobacter pylori* infection. *Helicobacter*, 2014, vol. 19, no. S1, pp. 1-5.
4. Park J.Y., Greenberg E. R., Parsonnet J., Wild C.P., Forman D. Summary of IARC working group meeting on *Helicobacter pylori* eradication as a strategy for preventing gastric cancer. *IARC Working Group Reports*, 2014, vol.8, pp. 1-181.
5. Sibille Y., Reynolds H.Y. Macrophages and polymorphonuclear neutrophils in lung defense and injury. *Am. Rev. Respir. Dis.*, 1990, vol. 141, no. 2, pp. 471-501.
6. Fialkow L., Wang Y., Downey G.P. Reactive oxygen and nitrogen species as signaling molecules regulating neutrophil function. *Free Radic. Biol. Med.*, 2007, vol. 42, no. 2, pp. 153-164.
7. Wiseman H., Halliwell B. Damage to DNA by reactive oxygen and nitrogen species: role in inflammatory disease and progression to cancer. *Biochem. J.*, 1996, vol. 313, pp. 17-29.
8. Hampton M.B., Kettle A.J., Winterbourn C.C. Inside the neutrophil phagosome: oxidants, myeloperoxidase, and bacterial killing. *Blood.*, 1998, vol. 92, no. 9, pp. 3007-3017.
9. Goldblatt D., Thrasher A.J. Chronic granulomatous disease. *Clin. Exp. Immunol.*, 2000, vol. 122, no. 1, pp. 1-9.

10. Baute J., Depicker A. Base excision repair and its role in maintaining genome stability. *Crit. Rev. Biochem. Mol. Biol.*, 2008, vol. 43, no. 4, pp. 239-276.
11. Lindahl T. Instability and decay of the primary structure of DNA. *Nature*, 1993, vol. 362, pp. 709-715.
12. Loeb L.A. Apurinic sites as mutagenic intermediates. *Cell*, 1985, vol. 40, no. 3, pp. 483-484.
13. Turgimbaeva A.M., Abeldenov S.K., Akhmetova D.G., Saparbayev M.K., Ramankulov Y.M., Khassenov B.B. Features of DNA repair mechanisms of man-infecting bacterial pathogens. *Eurasian J. Appl. Biotechnol.*, 2017, vol. 2., pp. 56-63.
14. A Ambur O.H., Davidsen T., Frye S.A., Balasingham S.V., Lagesen K., Rognes T., Tønjum T. Genome dynamics in major bacterial pathogens. *FEMS Microbiol. Rev.*, 2009, vol. 33, no. 3, pp. 453-470.
15. Abeldenov S., Khassenov B. Cloning, expression and purification of recombinant analog of Taq DNA polymerase. *Biotechnology. Theory and practice*, 2014, no. 1, pp. 12-16.
16. Maniatis T.F., Fritsch E.F., Sambrook J. Molecular cloning. A laboratory manual. New York: Cold Spring Harbor Laboratory, 1982, 545 p.
17. Joldybayeva B., Prorok P., Grin I.R., Zharkov D.O., Ishenko A.A., Tudek B., Bissenbaev A.K., Saparbaev M. Cloning and characterization of a wheat homologue of apurinic/aprimidinic endonuclease Ape1L. *PLoS One*, 2014, vol. 9, no. 3, p. e92963.
18. Ishchenko A.A., Sanz G., Privezentzev V.C., Maksimenko A.V., Murat Saparbaev M. Characterisation of new substrate specificities of *Escherichia coli* and *Saccharomyces cerevisiae* AP endonucleases. *Nucleic Acids Res.*, 2003, vol. 31, no. 21, pp. 6344-6353.
19. Abeldenov S., Talhaoui I., Zharkov D.O., Ishchenko A.A., Ramanculov E., Saparbaev M., Khassenov B. Characterization of DNA substrate specificities of apurinic/aprimidinic endonucleases from *Mycobacterium tuberculosis*. *DNA Repair*, 2015, vol. 33. pp. 1-16.
20. Takeshita M., Chang C.N., Johnson F., Will S., Grollman A.P. Oligodeoxynucleotides containing synthetic abasic sites. Model substrates for DNA polymerases and apurinic/aprimidinic endonucleases. *J Biol Chem.*, 1987, vol. 262, no. 21, pp. 10171-10179.
21. Kane C.M., Linn S. Purification and characterization of an apurinic/aprimidinic endonuclease from HeLa cells. *J. Biol. Chem.*, 1981, vol. 256, no. 7, pp. 3405-3414.
22. Rogers S.G., Weiss B. Exonuclease III of *Escherichia coli* K-12, an AP endonuclease. *Methods Enzymol.*, 1980, vol. 65, pp. 201-211.
23. Mathieu A., O'Rourke E.J., Radicella J.P. *Helicobacter pylori* genes involved in avoidance of mutations induced by 8-oxoguanine. *J. Bacteriol.*, 2006, vol. 188, no. 21, pp. 7464-7469.
24. Gros L., Ishchenko A.A., Ide H., Elder R.H., Saparbaev M.K. The major human AP endonuclease (Ape1) is involved in the nucleotide incision repair pathway. *Nucleic Acids Res.*, 2004, vol. 32, no. 1, pp. 73-81.
25. Tsutakawa S.E., Shin D.S., Mol C.D., Izumi T., Arvai A.S., Mantha A.K., Szczesny B., Ivanov I.N., Hosfield D.J., Maiti B., Pique M.E., Frankel K.A., Hitomi K., Cunningham R.P., Mitra S. T. Conserved structural chemistry for incision activity in structurally non-homologous apurinic/aprimidinic endonuclease APE1 and endonuclease IV DNA repair enzymes. *J. Biol. Chem.*, 2013, vol. 288, no. 12, pp. 8445-8455.
26. Mol C.D., Izumi T., Mitra S., Tainer J.A. DNA-bound structures and mutants reveal abasic DNA binding by APE1 DNA repair and coordination. *Nature*, 2000, vol. 403, no 6768, pp. 451-456.
27. Wong D., DeMott M.S., Demple B. Modulation of the 3'→5'-exonuclease activity of human apurinic endonuclease (Ape1) by its 5'-incised abasic DNA product. *The journal of biological chemistry*, 2003, vol. 278, no. 38, pp. 36242-36249.
28. Cunningham R.P., Weiss B. Endonuclease III (nth) mutants of *Escherichia coli*. *PNAS*, 1985, vol. 82, no. 2, pp. 474-478.
29. Blaisdell J.O., Wallace S.S. Abortive base-excision repair of radiation-induced

clustered DNA lesions in *Escherichia coli*. *PNAS*, 2001, vol. 98, no. 13, pp. 7426-7430.

30. Thomas D., Scot A.D., Barbey R., Padula M. B. Inactivation of OGG1 increases the incidence of G·C→T·A transversions in *Saccharomyces cerevisiae*: Evidence for endogenous oxidative damage to DNA in eukaryotic cells. *Mol. Gen. Genet.*, 1997, vol. 254, no 2, pp. 171-178.

31. Alseth I., Eide L., Pirovano M., Rognes T., Seeberg E., Bjørås M. The *Saccharomyces cerevisiae* homologues of endonuclease III from *Escherichia coli*, Ntg1 and Ntg2, are both required for efficient repair of spontaneous and induced oxidative DNA damage in yeast. *Mol. Cell. Biol.*, 1999, vol. 19, no. 5, pp. 3779-3787.

32. Ischenko A.A., Saparbaev M.K. Alternative nucleotide incision repair pathway for oxidative DNA damage. *Nature*, 2002, vol. 415, pp. 183-187.

33. Takeuchi M., Lillis R., Demple B., Takeshita M. Interactions of *Escherichia coli* endonuclease IV and exonuclease III with abasic sites in DNA. *J. Biol. Chem.*, 1994, vol. 269, nj. 34, pp. 21907-21914.